J Musculoskel Neuron Interact 2002; 2(6):592-602

Poster

Hylonome

Poster abstracts from the 32nd Meeting of the International Sun Valley Hard Tissue Workshop

4-8 August 2002, Sun Valley, Idaho, USA

Program Chairmen: W.S.S. Jee and D.B. Burr

Abstract No.	Topic
P1-28	Poster abstracts (Authors marked with an asterisk (*) are Young Investigator Travel Awardees)

P-1

Effect of Fracture and Immobilization in Bone Mineral Density and Mechanical Parameters in Postmenopausal Women With a Unilateral Distal Radius Fracture. Preliminary Report of an Ongoing Prospective Analysis.

P.J. Boscainos*, F.S. Giannoulis, P. Raptou, A. Galanos, G.P. Lyritis
Laboratory for the Research of the Musculoskeletal System, Medical School of the University of Athens, Athens, GREECE
E-mail: pbosc@panafonet.gr

Fracture of the distal radius is a relatively common incident in postmenopausal women that has been associated with postmenopausal bone loss. Moreover, a post-fracture decrease of bone mineral density has been attributed to immobilization and is considered to be a predictor for later fractures.

Seventeen postmenopausal women with a unilateral distal radius fracture with an indication for conservative treatment according to the universal classification of distal radius fractures were included in the study. Fracture alignment was achieved by manual manipulation and the forearm was stabilized with a 3M Scotchcast Plus casting tape (Minnesota, USA). pQCT measurements of the fractured forearm were performed 2-3 days after the fracture, at 10 days after the fracture and at cast removal (35-45 days). The non-fractured forearm was also measured at 10 days and at cast removal. All measurements were performed at a 10mm, 20mm and 40mm distance from a reference line set at the most proximal part of the distal radioulnar joint. Cortical, trabecular and total density and SSIx, SSIy and SSIpolar parameters were assessed. Paired t-test statistical analysis was performed using the SPSS package.

The mean age of the patient population was 66.9 (59-78) years and fracture occurred at a mean 18.3 (10-31) years after menopause. The dominant hand was involved in 8 patients and the mean immobilization period was 40.6 days. Fracture was classified as non-articular displaced (type 1) in 3 patients, non-articular displaced (type 2) in 11 patients and reducible, intra-articular displaced (type 4a) in 3 patients. No complications such as loss of reduction and evident complex regional pain syndrome were identified in this population.

At the fractured forearm, a high statistically significant decrease of cortical density was observed only between second measurement and cast removal at 10 and 20mm ($p<0.01$) At 40mm the differences were not significant ($p>0.1$). At 10 days after the fracture, cortical density difference of fractured and non-fractured forearm was not statistically significant at all distances ($p>0.1$). Total density was not significantly altered and trabecular density at 10mm was significantly increased at cast removal compared to values at the time of the fracture ($p<0.01$). Subcortical bone density at 10mm was also significantly decreased at cast removal ($p<0.01$).

At cast removal, SSIx and SSIpolar parameters of the fractured forearm were also statistically significantly decreased at distances of 10 and 20mm ($p<0.05$) but were not significantly decreased at 40mm. SSIy values on the other hand, at 10, 20 or 40mm, did not show statistically significant alterations.

Distal radius fractures in postmenopausal women treated with cast immobilization lead to a decrease of cortical density and an increase of trabecular density near the fracture site. They also aggravate bending and torsional mechanical properties. The shift from cortical bone to trabecular bone seems to be time-dependent and is significant at cast removal. Fracture healing and cast removal are not accompanied by restoration of bone density and mechanical properties of the fractured radius.

P-2

A Functional Role for EDR3 in Osteoblast Proliferation and Differentiation

*A.M. Deshpande[1], X. Reveles[2], R.G. Gorlick[3], P.A. Meyers[3], S.L. Naylor[2], R.J. Leach[2], M.F. Hansen[1]
[1] University of Connecticut Health Center, Farmington, CT, USA
[2] University of TX Health Science Center, San Antonio, TX, USA
[3] Memorial Sloan-Kettering Cancer Center, New York, NY, USA
E-mail: deshpando@nso2.uchc.edu

We have identified a novel homolog of the Drosophila Polyhomeotic gene, Early Development Regulator 3, (EDR3), which is a member of the Polycomb group (PcG) gene family. The EDR3 gene maps to human chromosome 3q26.2 - q26.3, spans 83.5 kb sequence and encodes a 983 aa protein. The mouse homolog, EDR3, is 92% identical to the human gene. We found that EDR3 was expressed widely during mouse development including the craniofacial region, the limbs, heart, liver and lungs. Immunohistochemistry revealed that EDR3 was expressed in the nuclei of the condensing mesenchyme in a punctate fashion. Further, when proliferating osteoblasts were induced to terminally differentiate *in vitro*, EDR3 was found to translocate to the nucleus where it resided in the same distinct punctate distribution. Members of the PcG family regulate gene expression through protein-protein and protein-DNA interactions and play an important role in axial patterning of organisms through regulation of homoetic gene expression. Co-localization and co-immunoprecipitation studies demonstrated that EDR3 interacts with other members of the PcG family and

the E2F6 transcription factor. These results suggest a functional role for EDR3 in regulation of proliferation and differentiation in osteoblasts.

P-3

Origins of Skeleton Pain: Sensory and Sympathetic Innervation of the Mouse Femur

K.J. Feia[1], D.B. Mach[1], S.D. Rogers[1], M.C. Sabino[1], N.M. Luger[1], M.J. Schwei[1], J.D. Pomonis[1], C.P. Keyser[1], D.R. Clohisy[2], D.J. Adams[3], P.O'Leary[2], P.W. Mantyh[1]
[1] University of Minnesota, Minneapolis, MN, USA & VA Medical Center, Minneapolis, MN, USA
[2] University of Minnesota, Minneapolis, MN, USA
[3] University of Connecticut, Farmington, CT, USA
E-mail: feia0003@umn.edu

Although skeletal pain plays a major role in reducing the quality of life in patients suffering from osteoarthritis, Paget's disease, sickle cell anemia and bone cancer, little is known about the mechanisms that generate and maintain this pain. To define the peripheral fibers involved in transmitting and modulating skeletal pain, we used immunohistochemistry with antigen retrieval, confocal microscopy and three-dimensional reconstruction of the bone to examine the sensory and sympathetic innervation of mineralized bone, bone marrow and periosteum of the normal mouse femur. Thinly and unmyelinated peptidergic sensory fibers were labeled with antibodies raised against calcitonin gene related peptide (CGRP) and the unmyelinated, non-peptidergic sensory fibers were labeled with the isolectin B4 (IB4, bandeira simplicifolia). Myelinated sensory fibers were labeled with an antibody raised against 200kD neurofilament H (clone RT-97). Sympathetic fibers were labeled with an antibody raised against tyrosine hydroxylase (TH). CGRP, RT-97, and TH immunoreactive fibers, but not IB4 positive fibers, were present throughout the bone marrow, mineralized bone and the periosteum. While the periosteum is the most densely innervated tissue, when the total volume of each tissue is considered the bone marrow receives the greatest total number of sensory and sympathetic fibers followed by mineralized bone and then periosteum. Understanding the sensory and sympathetic innervation of bone should provide a better understanding of the mechanisms that drive bone pain and aid in developing therapeutic strategies for treating skeletal pain.

P-4

DEXA-assessed BMC/LM Relationships in the Whole Body and Limbs of 3,500 Colombian Men and Pre- and Post-MP Women

C.C. Cure, G.R. Cointry, R.P. Cure, J. Romero, J.L. Ferretti
Osteolab & Universidad Metropolitana de Barranquilla, COLUMBIA
CEMFoC, Universidad Nacional de Rosario, ARGENTINA
E-mail: ferretti@idim.com.ar

Background: In whole-body studies with DEXA [Ferretti; Bone 22:683. 1998, n = 1,450] we had shown that 1. the densitometric mineral mass (BMC) correlated linearly with the lean mass (LM), and 2. that relationship showed similar slopes but decreasing intercepts in the order: pre-MP women > men > post-MP women > children.

These observations could be regarded as reflecting, respectively,

1. the homogeneous control of bone status by muscle strength in the species through the bone mechanostat, and 2. the interaction of sex hormones with that regulation.

Aims and Methods: This study aims to expand that evidence by analyzing a large sample of DEXA determinations of BMC, LM, and fat mass of 3,500 normal, Caucasic and Hispanic Colombian men and pre- and post-MP women.

This investigation also includes separate determinations of the same variables in the upper and lower limbs, as references for regions affected or not by gravity.

As previously observed for the whole body, the BMC data correlated logarithmically with fat mass data in all instances. Accordingly, they were analyzed both in crude form and after statistical adjustment to the mean fat mass values of the corresponding regions (Fat-adj.BMC).

Results: Interesting region-related differences were found between the intercepts of the curves.

- In the whole body, the crude-BMC / LM relationships were linear and parallel and showed the same intercept differences as previously observed, i.e., pre-MP women > men > post-MP women.
- In the lower limbs, the curves were also linear and parallel, but the differences were less significant than in the whole body and showed the decreasing order: pre-MP women > men = post-MP women.
- In the upper limbs, the relationships were also linear and parallel, but the intercept ranking was: men > pre-MP women > post-MP women.

After fat-adjustment of the BMC, the curves for the whole body remained linear and parallel, but the intercept for the men was similar to that of the pre-MP women. The order of the intercept magnitude in the limbs was always men >/= pre-MP women > post-MP women. The differences were more significant for the upper than the lower limbs.

Discussion: It can be assumed that LM is proportional to muscle mass, and that the fat-adjustment of the BMC (which deals with the perturbation induced by fat in the DEXA-BMC determination) renders this variable a more reliable indicator of the bone status than its crude values.

If so, then our results show that the sex-hormone-induced differences in the DXA-assessed muscle-bone proportionality in humans vary noticeably according to the region studied.

This variation could be related to differences in either the gender-specific morphogenetic conformation or the weight-bearing nature of the musculoskeletal structures in each limb, or both.

- In the **lower limbs**, women showed a higher BMC/LM proportionality than men. This may be related to the known, larger influence of body weight or fat on bone mass in adult females than males.

Supporting this interpretation, a higher position of the men's curve was observed after fat-adjustment of the BMC data in this skeletal region.

- This phenomenon could have also affected the behavior of the **whole-body** data.
- In the **upper limbs**, in which the skeletal strains come almost exclusively from muscle contractions, men's data always ranked higher in the graphs than women's did, regardless of the crude or adjusted expression of the BMC values.

Anthropometric differences between genders, especially concerning the hand skeleton (a region in which the bone/muscle proportionality is particularly high) could also contribute to explain that finding. Specific studies are needed in order to rule out the influence of the hands on the DEXA determinations of the muscle / bone proportionality in the upper limbs.

Despite the possible influence of anthropometric differences in the observed results, they also suggest that the well-known, positive effect of estrogens on the bone cells' response to biomechanical stimuli could be overcome by the much larger loads induced by muscles on the skeleton in men than women in selected skeletal regions.

Results evidence the importance of the regional muscles in the determination of bone mass, and the convenience to study muscles and bones at the same time. The developed graphs can be easily percentilized or z-scored as normal references for evaluation of the muscle-bone proportionality in men and especially in pre- and post-MP women. This could be a useful tool for assessing the involvement of disuse in the etiology of any type of osteopenias.

P-5

Effects of Growth Hormone (GH) on Bone Structure and on the Muscle-Bone Relationships in Hypophysectomized (Hx), Young Rats

S. Feldman, M.E. Leite Duarte, G. Cointry, R. Capozza, L. Sarrió, J. Romero, J.L. Ferretti
CEMFoC, Universidad Nacional de Rosario, ARGENTINA
Universidad Federal Fluminense, Rio de Janeiro, BRAZIL
E-mail: ferretti@idim.com.ar

Aims and methods: The skeletal effects of hormones are poorly understood because they are often studied disregarding the complete analysis of bone material, geometric and structural properties and the muscle-bone interactions. Aiming to describe biomechanically the musculoskeletal effects of GH, we studied 29 rats, either intact (9) or Hx at

15 days of age (20). The Hx animals were maintained otherwise untreated (Hx controls, 4) or were injected 30 (8) or 150 mIU/d of GH (BioSidus, Argentina) (8) (15) days after surgery for 45 days. Tetracycline labelling was performed 15 days before sacrifice. At the end of the study the femur diaphyses were scanned (pQCT, XCT-960, Stratec) in order to measure the vBMD, periosteal and endosteal perimeters, cortical thickness, CSA and bending moment of inertia (xCSMI) of the cortical cross-sections. The bones were then tested in 3-point bending at a slow deformation rate (1 N/min) and keeping the inter-support distance (L = 13 mm) constant. Load-deformation (W/d) curves were obtained showing the elastic and plastic periods separated by the yielding point (y), from which the yielding load and deformation (dy, Wy), the fracture load (Wf), the percentage of load supported in plastic conditions (100 [Wf-Wy] / Wf), and the diaphyseal stiffness (load / deformation at the yielding point, Wy/dy) were obtained graphically. The specific stiffness (elastic modulus, E) of the cortical tissue was indirectly calculated as Wy.L3 / 48.xCSMI. The gastrocnemius muscles were weighed immediately after dissection. The proximal tibial metaphyses were studied histomorphometrically.

Results: The Hx impeded the development of some 50% of the normal diaphyseal structural stiffness, strength, and proportion of resistance in plastic conditions. Treatment prevented 1/3 of the deficit in stiffness and 1/5 of that in strength at maximum (150 mIU/d dose) but failed to affect the plastic resistance. The two chief determinants of the diaphyseal bending stiffness and strength, namely, the intrinsic stiffness and the spatial distribution of the cortical bone (estimated by E and the xCSMI, respectively), were affected inversely by Hx. While E was strikingly enhanced by some 70% to over normal values in treated rats, the xCSMI values (as well as those of most of the other geometric indicators studied) were 75% lower than in the intact controls. The treatment prevented no more than 1/5 of the deficit in xCSMI and half of the deficit in cortical CSA, showing a clear dose / response proportionality. In contrast, it did not change the E values. The cortical vBMD (a partial determinant of E, together with other, microstructural factors not measured here, which also affect the plastic behavior of bones) was 17% reduced by Hx. Treatment prevented no more than half of that deficit, following a dose / response pattern. Histomorphometrically, Hx enhanced OS/BS and reduced MAR in tibial trabecular bone, while treatment improved both correlatively, and in association with the changes observed in the cortical vBMD. The gastrocnemius muscles lose 60% of their weight after Hx, and GH administration prevented only 1/5 of that loss at the maximum.

Further analyses and interpretation: Correlations between bone structural properties and their material or geometric determinants; between E, vBMD and histomorphometric data; between the bone geometric and material indicators, and between bone and muscle indicators, suggested:

1. that Hx delayed bone and muscle growth (the former slightly more than the latter), especially during the time elapsed since surgery until the beginning of treatment (15 days), showing no evidence catch-up afterwards;
2. that Hx reduced the cortical vBMD in association with an inhibition of the MAR and also with the delay in the development of muscle mass / strength;
3. that, despite (2), Hx strikingly augmented the intrinsic stiffness (E) of compact bone, an uncommon effect, rebel to treatment, and attributable to changes in the mineral-unrelated, microstructural determinants of that property;
4. that the combination of those effects disturbed the homeostatic control of bone design as a function of the stiffness of cortical bone tissue by the bone mechanostat (i.e., by inducing a shift in the mechanostat set point);
5. that Hx reduced the diaphyseal structural stiffness and strength as a result of its combined effects on both the bone geometric properties and the determinants of the plastic bone behavior (the excessive rigidity and the abnormal microstructural arrangement of the hard tissue, etc.), and
6. that GH, at the assayed doses, prevented the negative Hx effects on bone geometry and vBMD and on muscle development only partially, but it was little effective on the Hx-induced changes in the specific stiffness of bone tissue and in the whole-bone behavior in plastic conditions, a couple of features which could explain why the treatment failed in preventing the Hx-induced, severe delay in the achievement of the structural bone stiffness and strength.

The reasons for which Hx stiffened cortical bone tissue despite a reduction in its vBMD; the effects of larger GH doses on the same model, and the analysis of other Hx impacts on the studied variables remain to be established.

P-6

Tomographic (pQCT) Analysis of Bone Structure and Strength and Muscle-Bone Interactions in 15 Children with Osteogenesis Imperfecta (OI)

E.J.A. Roldán, J.L. Ferretti, G.R. Cointry, C. Tau
Calcium Metabolism Dept., Pediatric Hospital, Buenos Aires, ARGENTINA
E-mail: ferretti@idim.com.ar

Background, aims and methods: Bone strength is determined by both bone material properties and architecture. Bone material properties are determined by both matrix microstructure and mineralization and bone architecture is determined by both bone mass and distribution. Both bone microstructure and architectural properties are with time affected by the strength of the regional muscles.

pQCT can provide some indicators of relevant bone and muscle properties. The aim of this study was to assess 1. cortical vBMD and mass; 2. the influence of the regional muscles on those properties, and 3. the general impact of the assayed variables on bone strength in boys and girls affected by osteogenesis imperfecta (OI).

We have scanned the calf 66% site of 15 OI children aged 2-16 years (5 of each types I, III and IV) and a number of age-matched or slightly older controls.

Results: The volumetric density of cortical bone was either normal or subnormal in the OI children, with no definite evolution with age. Type IV children tended to show the lowest values. This effect would have resulted from a combination of an enhanced matrix mineralization and a high disuse Haversian remodeling rate.

Cortical vBMD was little affected by muscle CSA in controls but it decayed logarithmically with muscle mass in the OI children, from almost normal values at 400 m2 CSA or more down to very low values in extreme cases. Specific distribution regions for types I, III, and IV were shown.

Cortical vBMD had no significant impact on bone strength (as assessed by the fracture incidence) in the OI children, presumably because of their very poor bone microstructure.

The cortical bone mass (as assessed by the CSA) increased with age in controls and significantly less in type I OI children. Little or no development was shown by types III and IV.

The cortical bone CSA was closely associated to the fat-free (FF) muscle CSA in the normal boys and girls. The whole group of OI children showed a single, though lower slope. Different distribution zones were observed for types I, III, and IV.

The cortical bone CSA was a significant determinant of bone strength as assessed by its negative relationship with the Fx incidence rate in all the OI children as a whole.

A fairly good correlation was observed between the mobility score and the Fx incidence rate in the OI children, regardless of the OI type.

The correlation between the whole- and the FF-muscle CSA's showed similar slopes for control and type I OI children, while types III and IV showed a significantly lower slope.

Interpretation: In the OI children:

- Cortical vBMD was little or erratically affected, more in type IV, with practically no impact on bone strength.
- The development of cortical bone mass was severely affected, with a greater impact on bone strength than that of the cortical vBMD.
- Type III and specially type IV children showed very low values of all cortical bone mass, vBMD and strength, and muscle mass, while intermediate values were shown by type I, regardless of the gender.
- The strength of the regional muscles and the level of physical activity always improved all bone mass, vBMD and strength, more noticeably in type I than in types III and IV.
- An intrinsic compromise of the muscles may have affected bone health independently, especially in types III and IV.

P-7

Bone Histomorphometric Changes of Longitudinal Bone Growth in Mouse

A. Ito, N. Yamamoto, H.E. Takahashi
Niigata Bone Science Institute, Toyosaka City, Niigata, JAPAN
E-mail: akemi.ito@aiko.or.jp

Introduction: The mouse is widely used for *in vivo* animal experiments in bone fields. The histomorphometric study of growing animals has been difficult because it has a different process of bone activity such as modeling and remodeling. An understanding of mouse skeletal growth is essential to complete the experiment of bone histomorphometry.

Purpose: We examined the changes in tibial metaphysis in the growing C57BL/6J Mouse using histomorphometic analysis to characterize the longitudinal bone growth in C57BL/6J Mouse.

Material and Methods: Thirty C57BL/6J mice were serially sacrificed at 4, 12, and 24 weeks of age. All animals received subcutaneous injections of tetracycline and calcein at 4 and 2 days before sacrifice. Bone histomorphometric analyses were performed on undecalcified longitudinal sections of the proximal tibial metaphysis. Longitudinal growth rate(Lo.G.R), Growth plate width(G.Pl.Wi), Primary spongiosa width(Pr.Sn.Wi) were measured in this study.

Results:

Fig.1

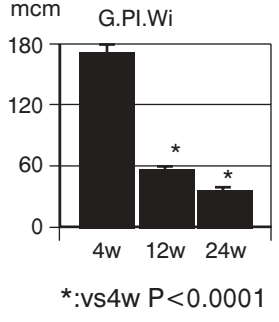

Fig.2

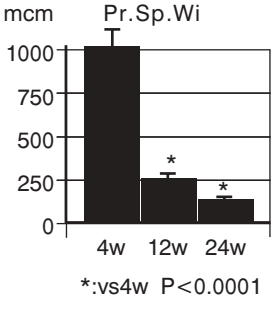

Fig.3

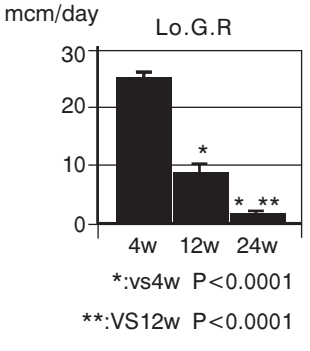

Discussion: Longitudinal bone growth was high at 4 weeks of age, about 25μm/day, but it was much smaller than that in the same age of rat. It gradually decreased with time and dropped to only 1μm/day at 24 weeks of age. Primary spongiosa width was 1000μm at 4 weeks, and it decreased to 100μmm at 24 weeks of age.

These data indicated that 6-month-old mouse growth plate remained open and still continued to grow longitudinally.

P-8

Genetic Variation in Cortical Bone Response to Ovariectomy in Three Inbred Mouse Strains

C. Li, M.B. Schaffler, H. Wolde-Semait, C. Hernandez, J. Ryan, J. Nadeau, K.J. Jepsen
Orthopaedic Research Lab., The Mount Sinai Hospital, New York, NY, USA
E-mail: chaoyang.li@mssm.edu

Effects of genetic background on the timing and magnitude of post-menopausal bone loss are not well understood. Inbred mice exhibit differences in bone formation rates during growth leading to differences in morphological and compositional traits of adult bone. It is reasonable to expect that inbred mice will also exhibit differences in response to ovariectomy (OVX). A total of 210 female 16-week-old mice from C3H/HeJ (C3H) (high density), C57BL/6J (B6) (low density), and A/J (intermediate density) inbred strains were examined. Ten mice from each strain were sacrificed at the beginning of the study. All other mice were either sham-operated (n=10/group) or ovariectomized (n=10/group), and sacrificed at 4, 8 and 16 weeks post-OVX. Differences in cortical bone mechanical properties were determined by loading femurs to failure in four point-bending. A/J femurs did not exhibit significant differences in maximum load at any time point following OVX. In contrast, B6 femurs exhibited a 10% reduction in maximum load at 4 and 8 weeks, and 20% at 16 weeks post-OVX compared to sham group. Maximum load in C3H femurs was lower at 4 (-7%) and 8 weeks (-12%) post-OVX compared to sham group, but caught up to the sham level at 16 weeks post-OVX. Our data to date reveal significant differences in the timing and magnitude of changes in cortical bone following OVX among three inbred mouse strains. These results suggest that genetic differences in peak bone properties do not predict the changes in cortical bone following OVX.

P-9

Investigation the Number of Mesenchymal Stem Cells (MSCs) and Gene Expression of Osteogenic Markers in Human Peripheral Blood Mononuclear Cells Isolated from Patients with Long Bone Fracture

G. Li, D. Shirley, G. Burke, D. Marsh
Queen's University of Belfast, Musgrave Park Hospital, Belfast, UK
E-mail: g.li@qub.ac.uk

Introduction: It is well established that the MSCs reside among the stromal compartment of bone marrow and can differentiate into functional osteoblasts under specific conditions. The presence of primitive haematopoietic cells in adult peripheral blood has been recognized for three decades. However, there is a long-standing controversy as to whether MSCs can migrate through the circulation. A few recent studies have suggested the existence of MSCs in adult guinea pig, mouse, rat and human peripheral blood, but there is no report on the presence of circulating MSCs during bone repair processes such as fracture. Utilising refined isolation procedures and molecular and immunohistochemical examinations, we examined the presence of osteoblastic and osteoprogenitor cells in peripheral blood of fracture patients and non-fracture controls. We investigated the expression of osteoblast differentiation related genes (alkaline phosphatase, osteocalcin, bone sialoprotein, Cbfa-1, BMP-2, -4, -6, BMPR1, BMPR2) and other genes related to signal transduction pathway activation (caveolin-1 and p90) in human blood mononuclear cells.

Methods: 30 ml of peripheral blood was taken from 5 healthy donors at one time point, and from seven patients with tibial or femoral fracture at 3 time points following fracture, days 1-3, 9-12 and 16-21. Patients were randomly selected, with mean age of 31, and presented with no known metabolic bone disease and were not under long-term medication. The peripheral blood mononuclear cells (PBMNCs) were isolated by centrifugation over a Lymphoprep density gradient (1.077 g/ml, Nycomed). 1/3 PBMNCs were immediately spanned onto glass slides and fixed, subject to immunocytochemistry (ICC) with various antibodies for phenotyping. 1/3 of PBMNCs were cultured in DMEM, supplemented with 10% FCS, antibotics, 50mg/ml ascorbic acid, 10 mM L-glycerophosphate, 10-8 M dexamethsone, at 37 0C in 5% CO2. Half of the medium was changed at 7 days and twice weekly thereafter. After 3 weeks, adherent cells were mobilized with trypsin/EDTA, and cultured in 8 well chamber slides for a week before they were fixed and used for ICC with various antibodies. RNA was extracted from the remaining 1/3 PBMCs within 4 hours of collection using the RNeasy Midi kit (Qiagen, UK). RNA integrity was verified by ethidium bromide staining of 28 S and 18 S ribosomal RNAs.

Gene expression of bone cell differentiation markers alkaline phosphatase, osteocalcin, bone sialoprotein, Cbfa-1, BMP-2, -4, -6, BMPR1, BMPR2, stromal derived factor (SDF) 1 and 2, and other genes including caveolin-1, p90/80K-H, VEGF, and the housekeeping genes acidic ribososmal protein (ARP) and b-actin was performed using semi-quantitative RT-PCR. Human osteoblastic cells derived from explants were used as positive controls in all experiments.

Results: The ICC results vary for the blood samples collected prior to cell culture. The PBMNCs in about two thirds of the blood samples from fracture patients showed the presence of positive staining for Cbfa-1, BMP-2, BMPR-I or II, Endoglin, Collagen type I, and Vimentin. In contrast, there was little or no staining of these markers in the PBMNCs from the controls. In the fracture patients' PBMNCs culture, numerous fibroblastic cells adhered to the flasks at the first week. The greatest number of adherent cells was found in the blood samples taken at 14-20 days post-fracture. After a period of 2 weeks, these cells were in spindle or round shapes, but did not form colonies in culture. ICC examinations confirmed that many of these culture-expanded cells were positive for Cbfa-1, BMP-2, BMPR-I or II, Endoglin, Type I collagen, Osteocalcin and Vimentin, but were negative for alkaline phosphatase. In contrast, we failed to observe any fibroblastic cell formation in the culture of PBMNCs from the controls, and the adherent cells at the end of the culture period were negative for most of the markers mentioned above.

For RT-PCR results, alkaline phosphatase mRNA expression in PBMCs was significantly unregulated in the PBMCs of fracture patients when compared with non-fracture controls at all time points following fracture. Bone sialoprotein and osteocalcin was only expressed in the osteoblast positive controls, but not detected in any of the PBMCs examined. Expression of BMP-2, -4 and -6 was observed in all cell types investigated, although there was considerable variation in the regulatory potential of the genes in the cells obtained from control volunteers and fracture patients. PBMCs demonstrated marked upregulation of BMP-2 gene in fracture patients in a time-dependent manner. BMPR1 was expressed in all PBMCs samples but BMPR2 was only expressed in the PBMCs of fracture patients. The expression of SDF-1 in PBMCs was negative but for SDF-2 was positive. Caveolin-1 and P90/80K-H (a phosphoprotein involved in the signal transduction pathway linked to the fibroblast growth factor 3 receptor) mRNA expression was significantly increased in PBMCs from fracture patients. PBMCs from fracture patients also expressed OSF-1 and Cbfa-1 to varying degrees. Housekeeping genes ARP and b-actin expression was unchanged between sample groups.

Discussion: This study has confirmed for the first time that patients with a recent fracture have an increase in the number of circulating MSCs in their peripheral blood. However, it is uncertain whether these circulating MSCs arise at the fracture site and leak into blood, or arise distally from the bone marrow or other sites in response to the fracture. Further study is on the way to clarify the links between trauma stimuli and the blood-borne MSCs. The gene expression of a number of osteogenic differentiation related markers, and genes implicated in signal transduction pathways, suggest a role for circulating cells in the peripheral blood contributing to the fracture healing process. Cells in the peripheral blood expressing BMP-2 may also contribute to the early induction of differentiation from mesenchymal cells to osteogenic cells. The identification of such precursor cells in blood may be of therapeutic significance, may contribute to the understanding of the bone repair process and suggest new treatment concepts for fracture and bone defects.

P-10

Different Tumors in Bone Each Give Rise to a Distinct Pattern of Skeletal Destruction, Bone Cancer-Related Pain Behaviors and Neurochemical Changes in the Central Nervous System

N.M. Luger, M.C. Sabino, D.B. Mach, S.D. Rogers, M.J. Schwei, K. Feia, P.W. Mantyh
University of Minnesota, Minneapolis, MN, USA and VA Medical Center, Minneapolis, MN, USA
E-mail: luger002@umn.edu

Pain is the most common presenting symptom in patients with bone cancer and bone cancer pain is often both debilitating and difficult to fully control. To begin to understand the mechanisms involved in the generation and maintenance of bone cancer pain, we implanted three well-described murine tumor cell lines, 2472 sarcoma, B16 melanoma and C26 colon adenocarcinoma into the femur of immunocompromised C3H-SCID mice. Although each of the tumor cell lines proliferated and completely filled the intramedullary space of the femur within three weeks, the location and extent of bone destruction, the type and severity of the pain behaviors, as well as the neurochemical reorganization of the spinal cord was unique to each tumor line injected. These data suggest that bone cancer pain is not caused by a single factor, but rather multiple factors are involved in generating and maintaining bone destruction and bone cancer pain. Understanding the factors that different tumors release to induce bone destruction and cancer pain should provide insight into the mechanisms responsible for the heterogeneity of bone cancer pain.

P-11

Imaging the Development of Bone Cancer Pain: Three-Dimensional Correlation of Tumor Growth, Osteoclast Proliferation, Bone Destruction and Activation of Sensory Neurons in a Murine Model of Bone Cancer

D.B. Mach[1], S.D. Rogers[1], M.D. Sabino[1], N.M. Luger[1], M.J. Schwei[1], K.J. Feia[1], J.D. Pomonis[1], D.R. Clohisy[1], D.J. Adams[2], P. O'Leary[1], P.W. Mantyh[1]
[1] University of Minnesota, Minneapolis, MN, USA VA Medical Center, Minneapolis, MN, USA
[2] Department of Orthopaedic Surgery, University of Connecticut, Farmington, CT, USA
E-mail: machx004@umn.edu

The most common symptom of bone cancer is pain. While bone cancer pain can induce a significant reduction in the patient's quality of life, little is known about the mechanisms involved in the generation and maintenance of bone cancer pain.

The aim of the present study was to build a 3-D model of the cells and molecules that contribute to bone cancer pain as tumor induced bone destruction progresses. Lytic sarcoma cells were injected into the intramedullary space of the mouse femur. Following tumor inoculation, animals were tested for ongoing and movement evoked pain. Bone density, formation and destruction were assessed using micro-computerized tomography and high-resolution radiographs. Tumor growth, osteoclast number and size, and sensory and sympathetic innervation were assessed and integrated into the 3-D bone images.

These data indicate rich sensory and sympathetic innervation of marrow, mineralized bone and periosteum. In mineralized bone the areas which receive the greatest stress and have the highest metabolic activity also receive the richest sensory and sympathetic innervation. These areas also show the greatest increase in osteoclast activation and show the earliest signs of tumor induced bone destruction. Understanding the sites, mechanisms and sequence by which tumor cells proliferate, promote bone destruction, induce osteoclast proliferation, and excite and destroy sensory and sympathetic fibers permits a better understanding of the factors that generate and maintain bone cancer pain.

P-12

Alendronate does not Prevent the Inflammation Reaction but Protects Bone from Resorption in a Rat Adjuvant Arthritis Model

Y.L. Ma, J.L. Hoover, Q.Q. Zeng, H. Cole, P. Shetler, C. Suen, H.U. Bryant
Gene Regulation, Bone and Inflammation Division, Lilly Corporate Center, Indianapolis, IN, USA
E-mail: ma_linda@lilly.com

The bisphosphonate alendronate is very well known for its potent anti-resorptive effect in bone. Since bone destruction is another major pathogenic change besides inflammation in rheumatoid arthritis, we examined the effect of alendronate in a rat adjuvant arthritis model. Male, 200g Lewis rats were injected with Lipoidal Amine 7.5 mg/kg at the base of the tail. At day 9,

dexamethasone (Dex) or alendronate treatment were initiated and continued for 5 days. Successful adjuvant arthritis was confirmed by the increase of paw weight. Histopathological evaluation of the tibiotarsal joint revealed dramatic inflammatory cell infiltration, extreme edema, fluid retention and periosteal proliferation. Significant bone resorption in association with numerous osteoclasts resulted in bone destruction and even distortion in both the calcanial and distal tibia metaphysis. Massive mesenchymal cells and inflammatory cells were also found in bone marrow. Faxitron X-ray showed significant soft tissue swelling, bone resorption, and even pathological fracture in the ankle joint. In contrast, treatment with Dex prevented the severe inflammation and bone resorption associated with this model. Paw weight, high resolution Faxitron X-ray image and histology evaluation showed no difference to the normal controls. Treatment with alendronate did not inhibit localized inflammation but prevented the bone resorption in the ankle joint. The paw and spleen weights were similar to the adjuvant arthritis controls. Faxitron X-ray showed an obvious swelling in the ankle joint, but the bone structures and density were normal. Histological evaluation revealed that although a similar inflammation change in soft tissue, much less mesenchymal cells were seen in marrow. Osteoclast number was only marginally increased and the calcaneal and distal tibial metaphyseal bone structure was intact when compared to the normal ankle joint. These data suggest that though alendronate does not alter the inflammation change, it has bone protective effects in this acute rat adjuvant arthritis model.

P-13

Difference of the Effects of Antiresorptive Agents on Fracture Repair of Ovariectomized Rats

S. Mori[1], Y. Cao[1], T. Mashiba[1], M.S. Westmore[2], L. Ma[2], M. Sato[2], T. Akiyama[1], L. Shi[1], S. Komatsubara[1], K. Miyamoto[1], H. Norimatsu[1]

[1] Kagawa Medical University, Kagawa, JAPAN

[2] Lilly Research Laboratories, Indianapolis, USA

E-mail: stmori@kms.ac.jp

Objective: Investigate the effects of antiresorptive agents on fracture repair in ovariectomized rats.

Methods: 140 female SD rats were either ovariectomized or sham-operated and divided into 5 groups: Sham (vehicle), OVX (vehicle), EE2 (0.1mg/kg,estrogen), Rlx(1.0mg/kg,raloxifene) and Aln(0.01mg/kg, alendronate). After 4 weeks treatment, pre-fracture controls were killed, while bilateral femura were osteotomized for remaining rats. Fracture calluses were excised at 6 and 16 weeks post-fracture for evaluation by radiography, QCT, biomechanical testing, and histomorphometry.

Results: At 6 weeks post-fracture, Aln and OVX had significantly larger calluses than other groups. Sham and OVX had significantly higher ultimate load than EE2 and Rlx, with Aln showing no difference from either control. Aln callus contained more mineral than all other groups. By 16 weeks post-fracture, OVX calluses were significantly smaller than at 6 weeks, while the callus volume for Aln had not changed. Aln had significantly higher BMC and ultimate load than OVX, EE2 and Rlx. EE2 and Rlx had similar biomechanical properties compared to Sham. Ultimate load normalized by body weight showed no significant difference among groups at either 6 or 16 weeks post-fracture. However, Aln strongly suppressed the callus remodeling, resulting in the lowest content of lamellar bone, persistent visibility of original fracture line.

Conclusions: OVX-stimulated bone turnover resulted in the fastest progression of fracture repair that was most delayed with alendronate. Estrogen and raloxifene had insignificant effects on fracture repair.

P-14

The Effects of Estrogen Deficiency on Monkey Mandibular Condyles Following Ovariectomy

*N. Ohashi[1], M. Tanaka[1], G. Lin[1], M. Ikegame[1], H. Tsusaki[2], K. Fukuzaki[2], S. Kohno[1], K. Hanada[1], S. Ejiri[1]

[1] Niigata University Graduate School of Medical and Dental Sciences, JAPAN

[2] Shin Nippon Biomedical Laboratories, Ltd., JAPAN

E-mail: ohashin@dent.niigata-u.ac.jp

Post-menopausal osteoporosis is an estrogen deficiency-caused state that causes severe bone loss in vertebrae and long bones. In the field of dentistry, the influence of estrogen deficiency on jaw bones has drawn attention, and the number of reports on this problem has increased yearly. Although the mandibular condyle plays an important functional role in mastication, fewer reports have been made on the mandibular condyle than on the mandibular body. Recently, there has been a report of bone mineral density (BMD) in human mandibular condyles being measured by computed tomography, and it was demonstrated that condylar bone mineral density decreased quickly after menopause, and was also correlated with spinal BMD[1]. We ourselves also have recently reported that there was region specificity of bone loss following ovariectomy (OVX) in the rat mandibular condyle. In the OVX rats, the bone volume in the posterior region of the condyle declined significantly, although no changes were found in the anterior region[2]. From a biomechanical standpoint, mechanical loading tends to occur more on the anterior region of the condyle than on the posterior. Furthermore, rat condylar movement consists mostly of an anteroposterior translation during mastication. However, condylar movement in humans is more multi-dimensional and complex. Therefore, monkeys were used in this experiment, as their masticatory jaw movement is similar to that of humans, in order to clarify more precisely how estrogen deficiency is correlated to bone loss in the condyles.

Twelve adult (over 9-year-old) female Macaca fascicularis monkeys were divided randomly into 2 groups of 6 subjects each. Under anesthesia, one group was ovariectomized bilaterally (OVX), while the others were given sham surgery (Sham) as controls. After surgery, periodic measurements were made of body weight and serum estrogen, as well as BMD of the lumbar vertebrae (LV) using DEXA. Seventy-six weeks after surgery, all subjects were sacrificed under anesthesia and the mandibles were excised. Horizontal condylar sections were made at a level 2mm below the superior tip of the condyle (Fig. 1a). The horizontal-plane areas of each of these cross-sections were divided into anterior and posterior regions, based on a dividing line drawn through the widest part of the condyle (Fig. 1b). The total, cortical and trabecular BMDs of the anterior and the posterior regions of the condyle were then analyzed, as well as that of the whole region. The comparisons among groups were done using one-way ANOVA, with the significance level at $p < 0.05$.

No significant differences in LV BMD were found between the OVX and Sham groups at the end of the experiment. However, the percentage decrement rate [(BMD at the end of the experiment/BMD at the beginning of the experiment) x 100%] of the LV in the OVX group was significantly greater in comparison with that of the Sham group.

In the anterior region of the condyle in the OVX group, total and trabecular BMDs were significantly lower than that of the Sham group ($p<0.05$). In the OVX group, the whole condyle as well as the posterior region in particular showed lower total and trabecular BMDs than that of the Sham group, without however being statistically significant. No significant differences between the OVX and Sham groups ware detected in cortical BMD in any of the regions inspected

This is the first report to analyze regional specificity of BMD in the condyle. One interesting result of this experiment was that it showed that even in an estrogen-deficient state, the mechanical loading stress caused by masticatory jaw movement seemed to reduce bone loss in the anterior cortical bone. On the other hand, the trabecular bone in the anterior region of the OVX condyle showed statistically greater bone loss than that of the Sham condyle. This might suggest that trabecular bone is more sensitive to the hormonal changes in comparison with cortical bone.

The total, cortical and trabecular BMDs in the posterior region of the condyle in the OVX group displayed no significant differences in comparison with those in the Sham group. One reason for this lack of statistically significant differences might be that a few of the condyles in the Sham group showed thin or irregular cortical bone in the posterior region of the condyle at the end of the experiment. These results suggest that the bone loss in the posterior region may have been the result of some other factors such as the influence of individual occlusal habit.

Therefore, the estrogen deficiency caused a region-specific BMD decrement in the monkey mandibular condyle, which may be attributed to the differences in mechanical loading by occlusion.

Acknowledgements

This work was supported by grants from the Ministry of Education, Science and Culture, Japan.

References

1. Yamada M, Ito M, Hayashi K, Sato H, Nakamura T. Mandibular condyle bone mineral density measurement by quantitative computed tomography: a gender-related difference in correlation to spinal bone mineral density. bone 1997; 21:441-445.
2. Tanaka M, Ejiri S, Kohno S, Ozawa H. Region-specific bone mass changes in rat mandibular condyle following ovariectomy. Dental Res 2000; 79:1907-1913

Figure 1.

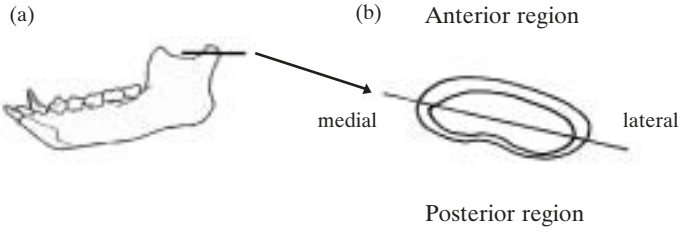

P-15

Molecular Characterization of Head and Neck Osteosarcoma Suggests a Distinct Disease Entity

*D. Pathmanathan, G. Pringle, E. McCarthy, K. Unni, M. Sanders, A. Deshpande, D. Ammerman, M. Hansen
University of Connecticut Health Center, Farmington, CT, USA
E-mail: dpathmanathan@up.uchc.edu

Osteosarcoma is the most common primary tumor of bone and the third most common malignancy in adolescents. Osteosarcoma of all sites accounts for approximately 20% of all malignant tumors of bone and approximately 7,500 new cases annually in the United States. Although a majority of osteosarcomas occur in the long bones of the skeleton, 6-13% of all osteosarcomas occur in the head and neck. Evidence from the differences in the degree of cellular atypia, the frequency of local versus distant metastases, the time until metastases, and the median age of onset, suggests that primary osteosarcoma of the appendicular skeleton and primary osteosarcoma of the head and neck represent biologically discrete diseases. To demonstrate this hypothesis, we chose to analyze expression patterns of genes implicated in appendicular osteosarcoma tumorigenesis. The expression patterns of these genes differed in head and neck osteosarcomas from those observed in the appendicular osteosarcomas. These results suggest that the mechanism of tumorigenesis in these two forms of osteosarcoma may also be distinct and that primary head and neck osteosarcoma may be a separate disease from appendicular skeletal osteosarcoma.

P-16

Consequences of Continued Exposure to PTH on the Regulation of AP-1 Genes and Osteoclast Induction

J. Milas, *N. Rao, S. Murthy, J. Pulcini, X. Yu, J.M. Hock
Indiana University School of Medicine, Indianapolis, IN, USA
E-mail: narao@iupui.edu

PTH has both anabolic and catabolic actions on bone. However, the mechanisms of actions are not well understood. The AP-1 family of genes coding for transcription factors has fundamental roles in osteoblast proliferation and differentiation, and is regulated by PTH. Our aims were to determine if there were divergent effects of PTH regimen on expression of AP-1 family genes *in vivo* and bone resorption, and if continued exposure to PTH *in vitro* modified proliferation or apoptosis of primary osteoprogenitors. Young C57Bl/6 male mice were treated for 5 days with vehicle or hPTH 1-34 at 40 μg/kg as 6 injections within 6-8 hours/day (which reduces BMD after 12 days, Black et al., JBMR 1994) and terminated 30min after the last injection. Femur metaphyseal RNA was pooled for each group and expression of selected AP-1 genes evaluated by RNAse protection assay. Mice were given calcein to label bone formation and BrdUrd to label proliferating cells. In experiment 2, mice were treated with vehicle or hPTH 1-34 at 40 μg/kg either once daily (intermittently) or with 6 injections/day (continuous) for 6 days to ascertain comparative effects of regimens. Bone marrow and spleen cells were cultured for 7 days with RANKL and M-CSF to assess TRAP+ multinucleated cells (osteoclasts). In experiment 3, apoptosis was measured in cultured primary bone marrow stromal cells exposed to hPTH 1-34 at 0-10-10M for 6h, 24h, 48h or 72h.

In vivo, continued exposure to PTH for 5 days initiated the catabolic response as urinary PYD/creatinine increased 1.4x and osteoclast number by 1.5x, although the time of treatment was not long enough for differences in bone mass to be detected. Immunohistochemistry showed an increase in BrdUrd+ fibroblasts and marrow fibrosis in the trabecular metaphysis of proximal tibia. Continuous PTH increased RNA expression of c-fos and junB, with little change in c-jun, junD or fra-2; the increase in c-fos expression was 3-fold less than that elicited by once daily PTH. *Ex vivo* induction of osteoclasts by continuous or once daily PTH increased osteoclasts respectively by 2.2x or 3.6x in bone marrow and by 1.5x or 1.6x in spleen precursors. *In vitro*, continuous exposure to PTH inhibited apoptotic caspase activity by 60% at 48h and 30% at 72h. Inhibition of osteoprogenitor apoptosis and *ex vivo* induction of osteoclasts did not depend on the regimen-dependent differences in c-fos expression. Comparisons of catabolic and anabolic PTH regimens suggest that the magnitude of increase in c-fos expression may regulate stromal progenitor cell choice of fate as osteoblasts or fibroblasts.

P-17

Mechanical loading imparts large increases in biomechanical strength despite only modest improvement in BMD in the rat ulna.

*A.G. Robling, F.M. Hinant, D.B. Burr, C.H. Turner
Indiana University School of Medicine, Indianapolis, IN, USA
E-mail: arobling@anatomy.iupui.edu

Mechanical loading of the skeleton increases bone mineral density (BMD). Mechanical loading also causes structural changes to the bone, not necessarily related to BMD. The goal of this study was to determine the effects of applied mechanical loading on the structure, areal BMD, and biomechanical properties of long bones in adult animals. We applied axial loading to the rat ulna *in vivo* three times a week for four months and quantified the changes in structural and mechanical properties, and in aBMD of the ulna. Twenty adult female Sprague Dawley rats were divided randomly into a loaded group (n=11) and an age-matched control (AMC) group (n=9). The right distal forearms of rats in the loaded group were subjected to 360 loading cycles per day in a single, uninterrupted bout. Loading sessions were conducted 3 days/week for 16 weeks. After sacrifice, the right and left ulnae were scanned using DXA and pQCT (for bone geometry). Subsequently, the bones were subjected to mechanical testing in axial compression. Rats subjected to 4 months of loading exhibited significantly greater IMIN in the right (loaded) ulnae when compared to the control (left) ulnae. The increase in IMIN was manifest along most of the diaphysis, reaching a 70% increase in the distal region. IMAX increased modestly as a result of loading. Mechanical properties were improved significantly by loading; ultimate force and work to failure were 70 and 83% greater, respectively, in the right arm of the loading group when compared to the right arm of the age-matched control group ($p<.001$ for both measurements). aBMD was increased by 5% due to loading ($p<0.05$). A strong correlation ($r=.94$) between bone strength and IMIN was found, suggesting that failure occurred in the IMIN (mediolateral) plane. The results demonstrate the potential of mechanical loading to improve structural properties in the mature rat ulna, and highlight the site specificity of the response along the length of the bone. Adaptation occurred almost exclusively in the plane of bending (mediolateral plane), which explains why such large increases in IMIN but not IMAX were observed, even with only a modest change in aBMD. aBMD was increased by only 5%, yet ultimate force and work to failure were improved by 70 to 83%. Thus, small increases in BMD can impart large increases in mechanical integrity if the new bone is distributed appropriately.

P-18

Osteoprotegerin Blocks Bone Cancer-Induced Skeletal Destruction, Skeletal Pain and Pain-Related Neurochemcial Reorganization of the Spinal Cord

M.J. Schwei, P. Honore, N.M. Luger, M.C. Sabino, S.D. Rogers, D.B. Mach, K.J. Feia, D.R. Clohisy, P.W. Mantyh
University of Minnesota, Minneapolis, MN, USA and VA Medical Center, Minneapolis, MN, USA
E-mail: schwe027@umn.edu

As advances in cancer detection and therapy have extended the life expectancy of cancer patients, increasing attention must focus on improving patients' quality of life. More than 1.2 million cases of cancer will be diagnosed in 2000 in the US alone. Approximately 30 to 50 percent of all cancer patients will experience pain and between 75 to 90 percent of patients with advanced cancer will experience significant, life-altering cancer-induced pain related to failed treatment and/or tumor progression. One of the most difficult to treat cancer pains is that related to cancer invasion of bone.

It has been established that most cancer-induced bone destruction is performed by osteoclasts, the body's principal bone-resorbing cell and it has recently been shown that the formation, survival, and bone-resorbing activity of these cells can be potently inhibited by the soluble tumor necrosis factor receptor family molecule osteoprotegerin (OPG). Herein, we utilize our recently developed murine model of bone cancer to study the development of bone cancer pain. In this model, cancer cells are injected into murine femora and within five days after injection, cancer-induced osteoclastogenesis and bone destruction begin.

Treatment with OPG (5 mg/kg/day, s.c.) blocked bone cancer-related pain behaviors, eliminated cancer-induced bone destruction and osteoclasts at sites of tumor, and markedly diminished peripheral sensitization of primary afferent fibers that are observed in animals with bone cancer pain.

These results demonstrate that excessive tumor-induced bone destruction plays a role in the generation of bone cancer pain and that osteoprotegerin may provide an effective treatment for this common human condition.

P-19

Alterations to the Cortical Bone Dynamics and Strength in the Elastase-Induced Emphysematous Hamster

*J.E. Shea[1], S.C. Miller[1], D.C. Poole[3], J.P. Mattson[2]
[1] University of Utah School of Medicine, Salt Lake City, UT, USA
[2] University of Utah, Salt Lake City, UT, USA
[3] Kansas State University, Manhattan, KS, USA
E-mail: j.shea@m.cc.utah.edu

Introduction: There is a growing body of evidence relating chronic obstruction pulmonary disease (COPD) to osteopenia and osteoporosis but the mechanisms linking these two diseases are unknown. The goal of the present investigation is to determine if there are alterations in cortical bone structure, dynamics, or strength in the elastase-induced emphysematous hamster model.

Materials and methods: Male Syrian Golden hamsters were divided into control (CON) and emphysema (EMP) groups and either saline (CON) or porcine elastase (EMP) instilled intratracheally. Calcien was administered via intraperitoneal injection 11 and 4 days prior to necropsy, which occurred three weeks following elastase injection. The right femurs were DEXA scanned and then loaded in three-point bending. The left femurs were embedded in methylmethacrylate and utilized for static and dynamic histomorphometric analysis.

Results: The EMP group had a 3% lower femoral bone mineral density, 6% lower femoral fracture strength, and 11% lower femoral stiffness compared to the CON group. Additionally, the resorption surface was 55% higher, the periosteal mineral apposition rate was 28% lower, and the cortical bone area was 27% lower than the CON group.

Discussion: The cortical bone exhibited rapid changes in bone formation and resorption, resulting in significant changes in bone structure and strength following the induction of emphysema. Systemic inflammatory cytokines, endocrine alterations, respiratory acidosis, and mechanical loading are all possible contributing factors in the observed skeletal changes. Future research needs to focus on elucidating the involved mechanisms connecting COPD, emphysema, and other chronic conditions with osteopenia.

P-20

Two Inbred Rat Strains That Differ Substantially in Hip Fragility

*Q. Sun, C.H. Turner
Indiana University School of Medicine, Indianapolis, IN, USA
E-mail: qisun@iupui.edu

One approach for identifying the genetic influences on skeletal phenotypes involves the creation and genetic mapping of a population of the second filial (F2) offspring derived from a cross of two inbred strains of rodents. The two inbred strains should be chosen based upon a large difference in the phenotype of interest, e.g. bone fragility. We found previously that considerable variation exists in fragility phenotypes among inbred strains of rats, and the phenotypic variation was site specific. In particular, two inbred rat strains, Copenhagen 2331 (COP) and Dark Agouti (DA), were found to differ significantly in femoral neck geometry and strength. The aim of this study was to further characterize hip fragility in COP and DA rats at six months of age using peripheral quantitative computed tomography (pQCT), microcomputed tomography (mCT), and biomechanical tests. COP rats had a significantly wider femoral head ($p=0.04$) and neck ($p=0.007$), significantly larger bone area and cortical bone area in femoral neck ($p=0.03$ and $p=0.02$, respectively), significantly higher total bone mineral content (BMC) and cortical BMC in femoral neck ($p=0.01$ and $p=0.001$, respectively), and also had 65% greater femoral neck cross-sectional moment of inertia ($p=0.02$), as compared to DA rats. As a result, COP rats had 22% higher ultimate force (Fu), 68% higher ultimate displacement (du), 81% higher work to failure (U) than DA rats in the femoral neck biomechanical test ($p=0.04$, $p=0.01$, and $p=0.02$, respectively). These data indicated that significant phenotypic variation at the femoral neck site exists between these two inbred strains, and COP rats appear to have genes that specifically enhance the femoral neck structural properties and strength. Therefore these two inbred strains, COP with DA, may facilitate effective genetic studies of hip fragility.

P-21

Effects of Age, Estrogen Depletion, and Parathyroid Hormone or Prostaglandin E2 Treatments on the Calcaneus in Ovariectomized Female Rats

*M. Su, W. Yao, X.Y. Tian, Y.F. Ling, *Q. Zhang, R.B. Setterberg, W.S.S. Jee
University of Utah School of Medicine, Salt Lake City, UT, USA
E-mail: mingsu98@yahoo.com; duweixin@yahoo.com

The main goals of this study were to determine age-related changes and estrogen-depletion effects on the calcaneus of rats and the envelope-specific responses of the calcaneus to parathyroid hormone (PTH) or prostaglandin E2 (PGE2) treatments. Female Sprague Dawley rats were subjected to sham surgery or bilateral ovariectomy at 6 months of age. Two months after surgery, ovariectomized (OVX) rats were injected subcutaneously (s.c.) for 60 days with vehicle or 80μg/kg hPTH(1-34) or with 6μg/kg PGE2. The calcaneus was collected from each rat and the mid-transverse sections were processed undecalcified for bone histomorphometry measurements.

In the calcaneus, periosteal expansion ceased at 6 months of age. Although periosteal bone formation and endosteal bone turnover were increased after OVX, neither cortical nor cancellous bone loss was observed. PTH and PGE2 treatments of OVX rats did not increase periosteal bone formation significantly. However, PGE2 increased the cancellous bone volume by 20% by thickening the trabeculae and increasing bone formation by nearly 300%. PTH treatment did not increase cancellous bone volume although the bone formation rate was increased by about 100% compared with vehicle treatment of OVX rats. These results indicate that the magnitude of anabolic responses to PTH and PGE2

treatments in calcaneus bone vary from those commonly seen in other cancellous bone sites such as the proximal tibial metaphysis and the lumbar vertebral body or cortical bone sites such as the tibial shaft. At these skeletal sites, augmented cancellous bone mass and markedly stimulated bone formation are generally observed with PTH treatment and stimulated periosteal bone formation is usually seen with PGE2 administration.

Groups	Ct.Ar %	BV/TV %	Ps-BFR µm/d	Es-BFR/BS $\mu m^3/\mu m^2/d$	Es-BFR/BV %/vr
Baseline	68±2	35±4	1.7±3.6	0.7±1.0	4.0±6.2
8mo-Sham	71±3	35±10	0±0	1.5±1.9	10.9±12.9
10mo-Sham	70±4	34±5	1.3±3.0	1.8±1.0	14.1±7.8*
8mo-OVX	74±2	30±4	17.8±8.7*#	4.2±2.6*	31.8±20.0*
10mo-OVX	74±5	35±4	0.5±1.3	6.3±9.7*	31.6±38.5*
PTH	72±3	34±12	5.8±6.1	13.4±4.4*#	80.0±30.3*#
PGE2	79±2*#	43±5*#	0.4±0.8	24.4±4.8*#	117.2±20.18*#

Mean ± SD; * = p < 0.05 vs. the baseline group; # = p< 0.05 vs. 10-mo OVX group; Ct. Ar, cortical bone area; Ps, periosteal bone surface; Es, endosteal surface (endocortical + cancellous bone surfaces); BFR, bone formation rate.

P-22

Rib Bone Strain and Muscle Activity in the Aetiology of Rib Stress Fractures in Rowers

*S.J. Warden,[1,2] D.A. Rath,[1] M. Smith,[1] H.G. Morris,[3] P.W. Hodges[4], F.R. Gutschlag[1]
[1] Australian Institute of Sport, ACT, AUSTRALIA
[2] Indiana University School of Medicine, IN, USA
[3] St Vincent's and Mercy Private Hospital, VIC, AUSTRALIA
[4] The University of Queensland, QLD, AUSTRALIA
E-mail: stwarden@iupui.edu

Rib stress fractures are a common and significant problem in the rowing population. However, little is known regarding their aetiology. The ribs are non-weightbearing. Therefore, rib stress fractures result from causes other than the forces associated with impact loading. The most frequently reported cause is the direct pull of muscle, with the serratus anterior (SA) and rectus abdominis (RA) muscles being the most commonly indicted. However, the role of these muscles in the aetiology of rib stress fractures is disputed. The aim of this study was to investigate the pattern of rib loading during rowing, and to compare this with the activity of muscles involved in the rowing stroke. The subject was a former elite level rower. Rib loading was assessed by attaching an instrumented bone staple to anterolateral aspect of the fifth rib. Muscle activity was assessed using fine-wire electromyography (EMG). Results showed that most rib loading occurred during the drive phase of the rowing stroke – a phase where SA and RA are minimally active. In comparison, the muscles predominantly active during the drive phase were the scapular retractor and the leg extensor muscles. Based on this finding, a novel mechanism for the aetiology of rib stress fractures in rowers is hypothesized.

P-23

Effects of Swim Training on skeletal Muscle and Bone in the Female Rat

*S. Warner, S. Doody, J. Shaw, S. Miller
University of Utah College of Health & School of Medicine, Salt Lake City, UT, USA
E-mail: swarner10@hotmail.com

Weight bearing is thought to have greater osteogenic potential than non-weight bearing activities. However, we have observed skeletal benefits with swim training in ovariectomized (OVX), retired breeder rats.

Purpose: To examine the effects of a 12-week swim training progression on skeletal muscle and bone in Sprague Dawley rats.

Methods: Forty female Sprague Dawley rats were weight-stratified into 4 groups (n=10 per group): sham control (SC), OVX control (OC), sham swim (SS), and OVX swim (OS). Rats were 120 days old and weighed 244 + 15 grams at study onset. Rats swam one hour per day, five days per week for twelve weeks. All rats were group housed and fed standard rat chow and water ad libitum. *In vivo* bone measurements of the proximal tibia (total, cortical, and trabecular mineral content (mg/mm), density (mg/mm2), and area (mm2)) were performed using pQCT XCT-960A (Stratec) at baseline and 12 weeks. Post necropsy four hind limb muscles were dissected and weighed, and the right humeri and femur were scanned by pDXA (Norland) to determine whole bone mineral content (BMC; g), density (BMD; g/cm2), and area (BA; cm^2).

Results: No group differences in body weight or bone existed at baseline ($p<0.05$). Body weight was significantly greater in OVX versus sham rats by week 2 and remained through week 12. Swimming increased total and cortical tibial bone mineral content ($p<0.05$). Three of four hind limb muscle weights were significantly higher in OS compared with SC ($p<0.01$). Humerus and femur BMD were significantly greater in the SS than OC.

Conclusion: Swimming increased some measures of bone density and skeletal muscle mass. Despite the insult of OVX, this model of a postmenopausal woman revealed an osteogenic response to swim exercise training.

P-24

Bone Histomorphometry of Iliac Cortical Bone in Osteitis Fibrosa (High Turnover Bone)

N. Yamamoto, A. Ito, H.E. Takahashi
Niigata Bone Science Institute, Toyosaka City, Niigata, JAPAN
E-mail: nirehp.yamamoto@aiko.or.jp

Introduction: Bone histomorphometry of human iliac bone biopsies provides important information in metabolic bone diseases. Renal osteodystrophy (ROD) has been classified by cancellous bone histomorphometry into two major groups, low turnover bone and high turnover bone. In this study we observed cortical bone changes in high turnover bone of ROD.

Material and methods: Bone biopsies were obtained from 4 patients with Chronic Renal Failure (average dialysis treatment period was 8.6 years). According to cancellous bone histomorphometry, they were diagnosed osteitis fibrosa (high turnover bone). Osteoid volume (OV/BV) 7.13±}2.58%, Fibrous tissue volume (Fb./TV)3.44±}2.23%, Bone formation rate (BFR/BV) 95.6±}35.38%.

Cortical bone histomorphometry of iliac bone specimen was performed using a semi-automated digitizing system (System Supply Co. Ltd., Japan). Mineral apposition rate(MAR), bone formation rate(BFR/BS), and eroded surface(ES/BS) were demonstrated in this study. (Table 1)

Results and discussion: Bone resorption was increased on both cancellous and all cortical surfaces. Cortical bone structure was disrupted by enlargement of Haversian canals and it made it difficult to distinguish two surfaces between endocortical and intracortical surfaces. It produced so-called cancellization of cortex. In conventional cortical bone histomorphometry, dynamic parameters are measured separately on two envelopes (endocortical surface, intracortical surface). Furthermore, the periosteal surface was not measured because it is supposed to be a resting surface in mature iliac bone. However in high turnover status like this study, all bone surfaces are activated, and sometimes it makes it difficult to define two surfaces (endocortical and intracortical) morphologically.

We propose that in osteitis fibrosa the whole cortical bone should be analyzed with cancellous bone.

	cancellous	endocortical	intracortical	periosteal
MAR (µm/day)	0.86±0.11	1.0±0.30	0.96±0.19	1.1±0.41
BFR/BS ($mm^3/mm^2/yr$)	0.072±0.028	-	0.034±0.015	0.094±0.046
ES/BS(%)	31.9±3.8	24.0±13.8	31.7±4.1	36.7±6.2

Table 1: Bone formation and resorption parameters in cancellous and cortical bone.

P-25

P2Y Purinergic Receptors are Necessary for Oscillatory Fluid Flow Induced Calcium Mobilization

IN OSTEOBLASTIC CELLS

*J. You[1], C. R. Jacobs[2], T. H. Steinberg[3], H. J. Donahue[1]
[1] The Pennsylvania State University College of Medicine, Hershey, PA, USA
[2] Stanford University, Stanford, CA, USA
[3] Washington University School of Medicine, St. Louis, MO
E-mail: jxy118@psu.edu

Recently fluid flow was shown to be a potentially important physical signal for mechanical loading-induced changes in bone cell metabolism. We previously demonstrated that oscillatory fluid flow activated MC3T3-E1 osteoblastic cell intracellular calcium (Ca^{2+}_i) mobilization via IP3 pathway in the presence of 2% FBS. The aim of this study is to investigate roles of extracellular signaling molecules and receptors on Ca^{2+}_i mobilization in response of oscillatory fluid flow. First we demonstrated that lacking extracellular signaling molecules (no FBS) osteoblasts failed to increase $[Ca^{2+}]_i$ in response to ±20dynes/cm^2 oscillatory fluid flow which suggests extracellular signaling molecules in FBS are required to activate Ca^{2+}_i mobilization. To search signaling molecule candidates, apyrase (10U/ml), an enzyme that rapidly hydrolyses 5' nucleotide-triphosphates to monosphophates, prevented an increased $[Ca^{2+}]_i$ in the presence of FBS. Meanwhile ATP or UTP (5mM), replacing FBS restored $[Ca^{2+}]_i$ responses which indicated that nucleotides ATP/UTP may be the signaling molecules induced by fluid flow. Next step, a series of ATP agonists and antagonists were employed to identify the receptors which are responsible for oscillatory fluid flow. Adenosine and ATPgS did not induce Ca^{2+}_i response under flow condition, and P2X/P2Y11 antagonist PPADS failed to prevent Ca^{2+}_i response which suggested P1 and P2X purinoceptors were not involved. Flow coming with ADP or UDP has little effect on Ca^{2+}_i implying P2Y1, P2Y6 and P2Y11 receptors did not play any role. Furthermore a selective G-protein inhibitor, PTX, completely blocked flow effect on MC3T3-E1 cells, again suggesting G-protein coupled P2Y receptors response for signaling. Thus, by a process of elimination, our data suggest that P2Y receptors (P2Y2 or P2Y4) are involved in the Ca^{2+}_i response to fluid flow. Finally, MC3T3-E1 osteoblastic cells treated with P2Y2 antisense oligodeoxynucleotides decreased the percentage of cells responding to fluid flow with an increase in $[Ca^{2+}]_i$ and ROS 17/2.8 osteoblasts transfected with P2Y2 purinoceptors increased the percentage of cells responding in the presence of 2% FBS confirming that P2Y2 purinoceptors are responsible for oscillatory fluid flow to induce Ca^{2+}_i mobilization. Our finding is the first direct experimental evidence showing that fluid flow and the extracellular signaling molecules ATP/UTP with their specific P2Y receptors are essential regulators for bone cell mechanotransduction.

P-26

CONSTITUTIVE ACTIVATION OF RAS SIGNALING INCREASED OSTEOPONTIN EXPRESSION AND IMPAIRED BONE STRENGTH, BUT NOT BONE MASS IN A MOUSE MODEL OF NEUROFIBROMATOSIS TYPE 1

*X. Yu, J. Milas, S. Murthy, D.W. Clapp, S. Chen, J.M. Hock
Indiana University School of Medicine, Indianapolis, IN, USA
E-mail: xijyu@iupui.edu

Impaired bone healing and osteoporosis occur in up to 50% of humans with Neurofibromatosis Type 1 (NF1). The loss of neurofibromin, which negatively regulates p21-ras, in NF1 results in constitutive activation of ras signal transduction. A study of Nf1 heterozygote mice (*Nf1* +/-), which exhibit several features of human NF1, offers a unique opportunity to understand how impaired ras signaling affects bone *in vivo*. Our goals were to define the skeletal phenotype and determine if any of the human bone problems were present in the mice. The skeletal phenotype was defined as bone mass, bone strength and bone histomorphometry. Cell biology was characterized as proliferation, apoptosis, osteoblast commitment (ALP+ CFU-f) of metaphyseal bone cells and diaphyseal bone marrow stromal cells, and *ex vivo* induction of osteoclasts (TRAP+ multinucleated cells) from spleen or bone marrow cells exposed to RANKL and M-CSF. Molecular characterization was based on RT-PCR of selected proteins in whole bone, metaphyseal bone cells and bone marrow stromal cells. Bone mass (BMD, BMC, XA and ash weight) and trabecular bone histomorphometry were equivalent in *Nf1*+/- and intact control mice. In female Nf1+/- mice, biomechanical properties of strength (ultimate force and stiffness) were impaired. In male *Nf1*+/- mice, cortical bone formation decreased but there was no detrimental effect on male bone strength. Osteoprogenitor proliferation, apoptosis and osteoblast commitment were all significantly impaired in *Nf1*+/- mice, while *ex vivo* induction of osteoclasts was increased and further enhanced by PTH and $1,25(OH)_2D_3$. RT-PCR showed that osteopontin (OPN) expression increased, but only in bone marrow stromal cells. OPN expression in whole bone, metaphyseal bone cells and osteoclasts was equivalent to control. Immunohistochemistry showed increased OPN in whole bone of *Nf1*+/- mice, especially where bone metabolism was active. mRNA Expression of type I collagen, alkaline phosphatase, PTH1R, RANKL and osteoprotegerin was equivalent in whole bones and primary bone cells from *Nf1* +/- mice and intact controls. As bone marrow stromal cells support both osteoblast and osteoclast function, altered OPN due to haploinsufficiency of *Nf1* may perturb bone cells homeostasis, resulting in detrimental effects on biomechanical properties of bone strength. Our next goal is to determine if the changes in OPN expression correlate with the impaired bone fracture healing known to occur in *NF1* children.

Acknowledgment

This work was supported by National Neurofibromatosis Foundation and US Dept Defense Neurofibromatosis Research Program.

P-27

OSTEOPROTEGERIN INHIBITS PROSTATE CANCER-INDUCED OSTEOCLASTOGENESIS AND PREVENTS PROSTATE TUMOR GROWTH IN THE BONE OF MICE

*J. Zhang[1], J. Dai[1], Y. Qi[2], D-l. Lin[1], P. Smith[1], C. Strayhorn[3], A. Mizokami[4], Z. Fu[1], J. Westman[3], E. T. Keller[1]
[1] University of Michigan School of Medicine, Ann Arbor, MI, USA
[2] Tianjin 3rd Municipal Hospital, Tianjin, CHINA
[3] School of Dentistry, University of Michigan, Ann Arbor, MI, USA
[4] Kanazawa University School of Medicine, Kanazawa, JAPAN
E-mail: jzhangqi@umich.edu

Prostate cancer (CaP) forms osteoblastic skeletal metastases with an underlying osteoclastic component. However, the importance of osteoclastogenesis in the development of CaP skeletal lesions is unknown. In the present study, we demonstrate that CaP cells directly induce osteoclastogenesis from osteoclast precursors in the absence of underlying stroma *in vitro*. CaP cell production of a soluble form of the osteoclastogenic protein, receptor activator of NFkB ligand (RANKL), was found to account for the CaP-mediated osteoclastogenesis. To evaluate for the importance of osteoclastogenesis on CaP tumor development *in vivo*, CaP cells were injected both intratibially and subcutaneously in the same mice, followed by administration of the decoy receptor for RANKL, osteoprotegerin (OPG). OPG completely prevented establishment of mixed osteolytic/osteoblastic tibial tumors that were observed in the vehicle-treated animals, but had no effect on subcutaneous tumor growth. Consistent with the role of osteoclasts in tumor development, osteoclast numbers were elevated at the bone:tumor interface, but at normal numbers in bone from OPG-treated mice. Furthermore, OPG had no effect on CaP cell viability, proliferation, or basal apoptotic rate *in vitro*. These results emphasize the important role that osteoclast activity plays in the establishment of CaP skeletal metastases, including those with an osteoblastic component.

P-28

LONGITUDINAL CHANGES IN 3D TRABECULAR MICROARCHITECTURE OF PAIRED ILIAC CREST BONE BIOPSIES BEFORE AND AFTER ESTROGEN REPLACEMENT THERAPY IN POSTMENOPAUSAL WOMEN

*J. Zhao[1], Y. Jiang[1], S. Vedi[2], J.E. Compston[2], H.K. Genant[1]
[1] University of California,at San Francisco, San Francisco, CA, USA
[2] University of Cambridge, Cambridge, UK
E-mail: jenny.zhao@oarg.ucsf.edu

Postmenopausal bone loss is associated with deterioration of trabecular bone microarchitecture, which has adverse biomechanical effects. Estrogen

replacement therapy (ERT) has been shown to prevent menopausal bone loss and reduce fracture risk, but its effects on three-dimensional (3D) trabecular microarchitecture have not been characterized. This study was designed to capture true longitudinal changes in 3D trabecular architecture before and after ERT, which may improve our ability to estimate bone biomechanical properties in terms of fracture resistance, as the mechanical competence of trabecular bone is a function of its apparent density and 3D distribution. During aging and in diseases such as osteoporosis, trabecular plates are perforated and connecting rods dissolved, with a continuous shift from one structural type to the other. These changes can not be evaluated by 2D histological sections in bone histomorphometry based on the parallel plate model assumption. We examined paired bone biopsies from the iliac crest (not a primary weight bearing anatomical site) from 20 postmenopausal women with osteopenia or osteoporosis. Bone biopsies were obtained from one side of the iliac crest before treatment and from the other side after treatment (mean 2 years). The specimens were blindly scanned and evaluated using a micro computed tomography scanner (BCT 40, Scanco) with isotropic resolution of 15 Bm3. 3D trabecular structural parameters were directly measured without stereological model assumptions as in 2D histomorphometry. Values of 0 and 3 for the structure model index represent an ideal plate structure and a perfect cylindrical rod structure, respectively, while values between 0 and 3 indicate a structure with both plates and rods of equal thickness, depending on the volume ratio of rods and plates. Compared with pre-treatment, post-treatment biopsies showed significant change in structure model index (-13.7%). Post-treatment changes in 3D trabecular bone volume fraction (+0.3%), trabecular thickness (+2.4%), trabecular number (-13.2%), trabecular separation (+9.0%), connectivity density (-0.4%), and degree of anisotropy (-4.4%) were statistically non-significant. The results indicated that ERT not only preserves existing 3D trabecular bone microarchitecture and connectivity but also is able to reverse the change from rod-like structure to plate-like pattern, which may improve trabecular biomechanical competence in terms of resistance to osteoporotic fragility fractures.